

## Dynamic Response of a SDOF system subjected to simulated downburst winds

Michael Chay<sup>1)</sup> and Faris Albermani<sup>2)</sup>

<sup>1), 2)</sup> *Department of Civil Engineering, University of Queensland, St Lucia QLD 4072*

<sup>1)</sup> *m.chay@uq.edu.au*

### ABSTRACT

This study provides an investigation of the dynamic response of a Single Degree Of Freedom (SDOF) structure subjected to simulated downburst winds. Wind speed time histories were simulated using an analytical model of a downburst wind field and an Autoregressive Moving Average (ARMA) turbulence simulation (Chay et al 2005). A variety of turbulence and damping conditions were investigated. The structure is a simple spring-mass-damper system. The investigation was conducted in the time domain using a direct numerical integration of the equations of motion (Paz 1997).

The response of the system under the action of the downburst winds is compared to that of the same system subjected to simulated boundary layer winds. The paper also presents an investigation of the affect that various downburst traits, such as the radius to maximum velocity and storm direction, have on the dynamic response.

Finally, a case study is presented which examines the dynamic response of the SDOF system when subjected to a simulation of the 1983 Andrews Air Force Base downburst (Fujita 1990).

### INTRODUCTION

Downbursts are now a recognised cause of design wind speeds in many regions around the world, and have also been responsible for numerous structural failures in recent times. Although downbursts are a relatively recently discovered phenomenon, modelling and simulation techniques have now reached a point at which we may start to examine the response of structures subjected to such events. However, prior to dynamic investigations of complex, Multiple Degree of Freedom systems, there is value in first investigating the response of simple structures to gain an insight into what variations there might be in the way in which more complex systems may act under the action of a downburst in comparison to boundary layer winds.

### EXPERIMENTAL CONFIGURATION

#### SDOF System

The structure under scrutiny during this study can be conceptualised as a SDOF 'Spring-mass-damper' system, shown in Figure 1. The structure is linear-elastic. Natural frequency ( $f_n$ ) was varied between 0.05Hz and 4.8Hz by altering the mass ( $m$ ) associated with a 100kN/m spring stiffness ( $k$ ). The damping ( $c$ ) of the structure was expressed in terms of the critical damping ratio ( $\xi$ ).

Force time histories throughout this study have been created from simulated wind speed time histories, using Equation (1):

$$F(t) = \frac{1}{2} \rho U(t)^2 C_d A \quad (1)$$

where  $\rho$  is the air density ( $1.2 \text{ kg/m}^3$ ), and  $U(t)$  is the wind speed at time  $t$ . The  $C_d A$  (drag coefficient times area) value of the structure was arbitrarily chosen as 2.4.

### Time Domain Dynamic Analysis

The equations of motion for the SDOF system were solved in the time domain using a direct numerical integration outlined by Paz (1997). This method assumes that force varies linearly between points in the loading time history.

### Wind Speed Time History Generation

A variety of techniques were used to generate the wind speed time histories during this study, including Computational Fluid Dynamics (CFD) and Autoregressive Moving Average (ARMA) methods. The methods used to generate the downburst wind speed time histories are described in detail in Chay et al (2005). A summary is provided here.

The downburst wind speed time histories were generated as the sum of the non-turbulent and turbulent components (Equation (13)), which are both functions of location and time.

$$U(x, y, z, t) = \bar{U}(x, y, z, t) + u'(x, y, z, t) \quad (2)$$

where  $U(x, y, z, t)$  is the total wind velocity;  $\bar{U}(x, y, z, t)$  is the non-turbulent wind velocity; and  $u'(x, y, z, t)$  is the turbulent fluctuation.

The non-turbulent wind speeds were simulated first, using a modified version of an analytical model of the downburst wind field. The analytical model used takes the form:

$$\bar{U}_r(x, y, z, t) = \Pi \frac{\bar{U}_{r, \max} r}{r_t} \frac{\left[ e^{c_1(z/z_r)} - e^{c_2(z/z_r)} \right]}{\left[ e^{c_1} - e^{c_2} \right]} e^{\left[ \frac{1 - (r^2/r_t^2)^\alpha}{2\alpha} \right]} + \bar{U}_{Trans} \quad (3)$$

$$\bar{U}_z(x, y, z, t) = -2\Pi \frac{\bar{U}_{r, \max} z_m}{r_p} \frac{\left\{ \frac{1}{c_1} \left[ e^{c_1(z/z_r)} - 1 \right] - \frac{1}{c_2} \left[ e^{c_2(z/z_r)} - 1 \right] \right\}}{\left[ e^{c_1} - e^{c_2} \right]} \left[ 1 - \frac{1}{2} \left( \frac{r^2}{r_t^2} \right)^\alpha \right] e^{\left[ \frac{1 - (r^2/r_t^2)^\alpha}{2\alpha} \right]} \quad (4)$$

where  $\bar{U}_r$  is the radial non-turbulent velocity,  $\bar{U}_z$  is the vertical non-turbulent velocity,  $\Pi$  is the intensity factor,  $\alpha$ ,  $c_1$ , and  $c_2$  are model constants (equal to 2, -0.15 and -3.2175 respectively),  $r$  is the radius to the point of observation in the horizontal plane from the centre of the storm ( $r = (x^2 + y^2)^{0.5}$ ),  $z$  is the elevation above ground level to the point of observation,  $r_t$  is the time dependent radius to maximum velocity,  $z_m$  is the height of maximum wind speed at  $r_t$ ,  $\bar{U}_{r, \max}$  is the desired maximum radial speed, and  $\bar{U}_{Trans}$  is the storm translation speed. An example of the wind speed profiles produced by this model is shown below in Figure 2.

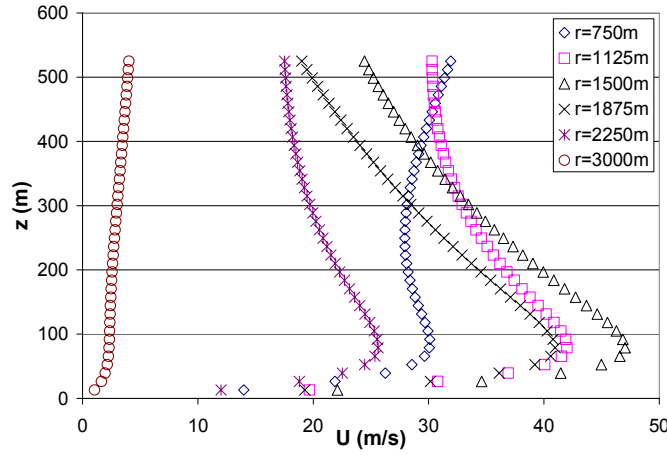


Figure 2: Wind Speed profile produced by the analytical model for simulating non-turbulent wind speeds in a downburst

Turbulence was added to the simulations using an ARMA process. A correlated Gaussian time history,  $\kappa(x,y,z,t)$ , with a mean of zero and a variance of 1 was generated based on the Kaimal Spectrum (Kaimal et al 1972), using a roughness height of 0.02m, and an elevation above ground level of 10m. The full methodology for the ARMA method used can be found in Samaras et al (1985). The time history is then amplitude modulated to the appropriate intensity using Chen and Letchford's (2004) method of multiplying by a ratio of the non-turbulent wind speed:

$$u'(t) = a(x,y,z,t)\kappa(x,y,z,t) \quad (5)$$

In this study  $a(x,y,z,t)$  was varied between  $0.01 \bar{U}(x,y,z,t)$  and  $0.25 \bar{U}(x,y,z,t)$ .

Similarly boundary layer like winds were generated by selecting a mean wind speed, and applying turbulence in the manner described above. Although this creates a somewhat artificial situation, whereby the boundary layer turbulence does not necessarily correspond to that which would be observed in nature for the same roughness height, mean speed and elevation, it facilitates easier comparison between the various simulated events.

In this study,  $\kappa(x,y,z,t)$  was generated based on the same spectral density function for both the downburst and boundary layer winds to eradicate any change in response due to variation in the properties of the Gaussian time history due to the turbulence spectrum type. The assumption that downburst winds exhibit turbulence that matches the Kaimal Spectrum is unproven. Certainly, there is preliminary evidence to suggest that there may be differences. Choi and Hidayat (2002) observed turbulence that showed different spectral density functions to those of boundary layer winds in Singapore. However, their analysis process did not employ any amplitude modulation of turbulence, making their results difficult to compare directly to this study. Chen and Letchford (2005) suggested

$$S_u(\omega, z) = \frac{\sigma(z)^2}{2\pi} \left\{ \begin{array}{l} [1 - \phi_2(z)]^2 + \phi_1(z)^2 \\ + 2\phi_1(z)[1 + \phi_2(z)]\cos\omega \\ + 4\phi_2(z)\cos^2\omega \end{array} \right\} \quad (6)$$

where  $\sigma(z)$ ,  $\phi_1(z)$ ,  $\phi_2(z)$  are functions that varied between the events observed. Turbulence generation was performed at 5Hz.

A variety of scenarios were investigated, however in all cases the peak gust speed during all events was  $50 \pm 2.5$  m/s. While it would be more traditional to select a mean speed and desired turbulence intensity, it is somewhat more difficult to apply this kind of selection process to a downburst. Due to the transient nature of downbursts, mean speed has little meaning. The most tangible quality that we can extract from our current record of severe wind speeds is the gust speed, and hence this was used as a means of selecting simulated events.

## TESTING AND RESULTS

### Response under Boundary Layer Winds versus Downburst Winds:

The first stage of testing involved subjecting the structure to boundary layer (BL) style wind conditions. A variety of turbulence intensities were considered. They are listed below in Table 1 with the corresponding mean speeds required to create a  $50 \pm 2.5$  m/s gust speed.

Table 1: Mean speed versus turbulence intensity for the boundary layer simulations.

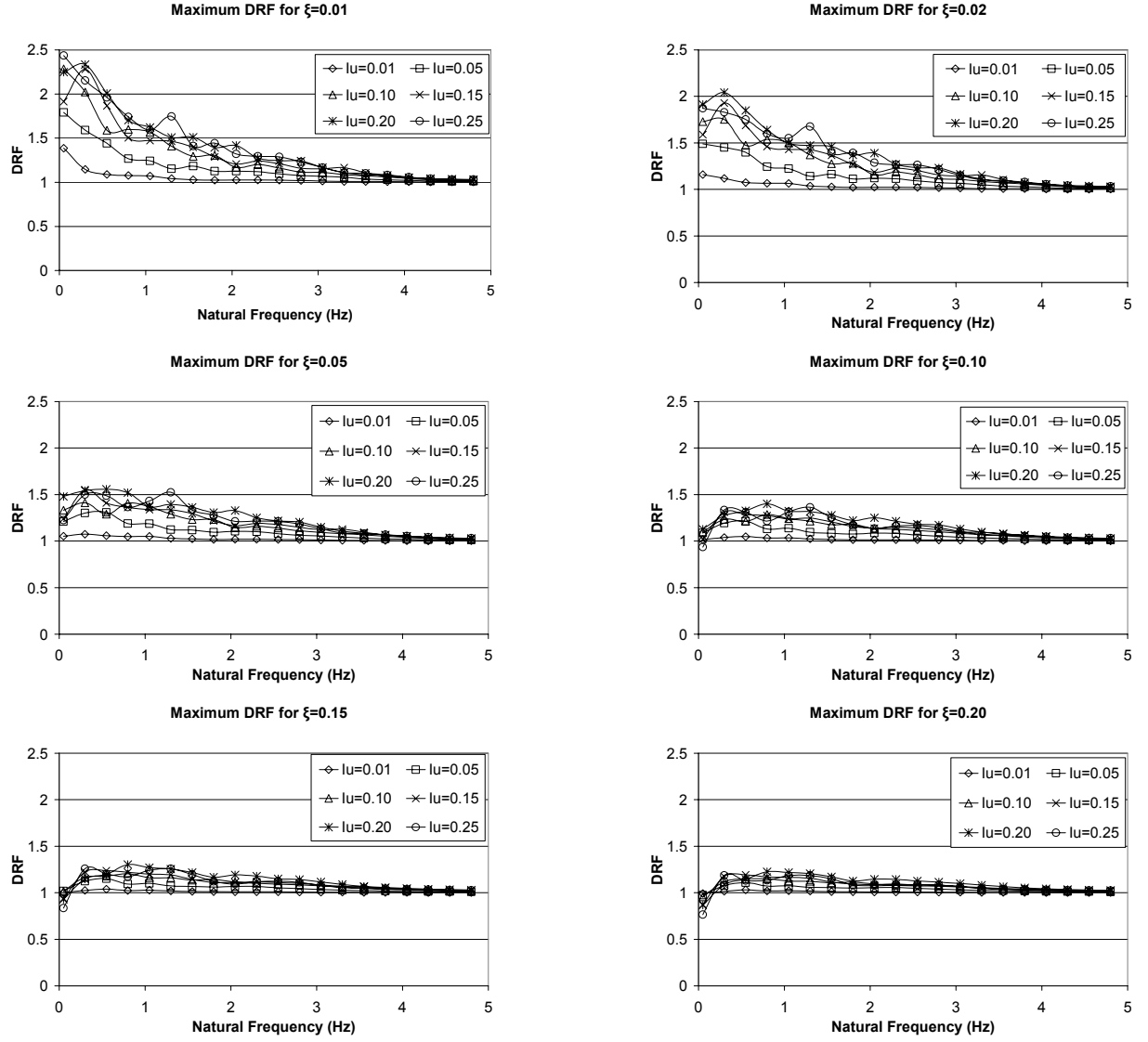
Turbulence Intensity (Iu)	Mean Speed (m/s)
0.01	49
0.05	48.5
0.10	37
0.15	32.5
0.20	29.5
0.25	26.5

For each turbulence intensity, twenty storm events meeting the gust speed threshold described above were generated. Each simulated time history was 20 minutes long. However, only the middle 10 minutes of the simulation was given consideration, to avoid errors associated with initial conditions and so that the duration was of a similar length to the downburst events considered throughout the study.

Wind speed time histories were converted to 25Hz resolution by linearly interpolating between points in the original time history, which was generated at 5Hz. The 25Hz wind speed time histories were then converted to wind loading time histories, using equation (1). The loading time histories were applied to the structure for a range of critical damping ratios from  $\xi=0.01$  to  $\xi=0.20$ , and natural frequencies between  $f_n=0.05$ Hz and  $f_n=4.8$ Hz in increments of 0.25Hz. For each event, damping ratio and natural frequency, a Dynamic Response Factor (DRF) was calculated from the displacement time history of the structure. The DRF in this case is defined as the largest dynamic displacement divided by the static displacement caused by the largest force:

$$DRF = \frac{S_{\max, dyn}}{F_{\max}/k} \quad (7)$$

At each damping ratio and natural frequency the largest of the DRFs for the twenty test storms was selected, and an ensemble average of DRF was calculated for all twenty storms. The results for the boundary layer style winds are shown below:



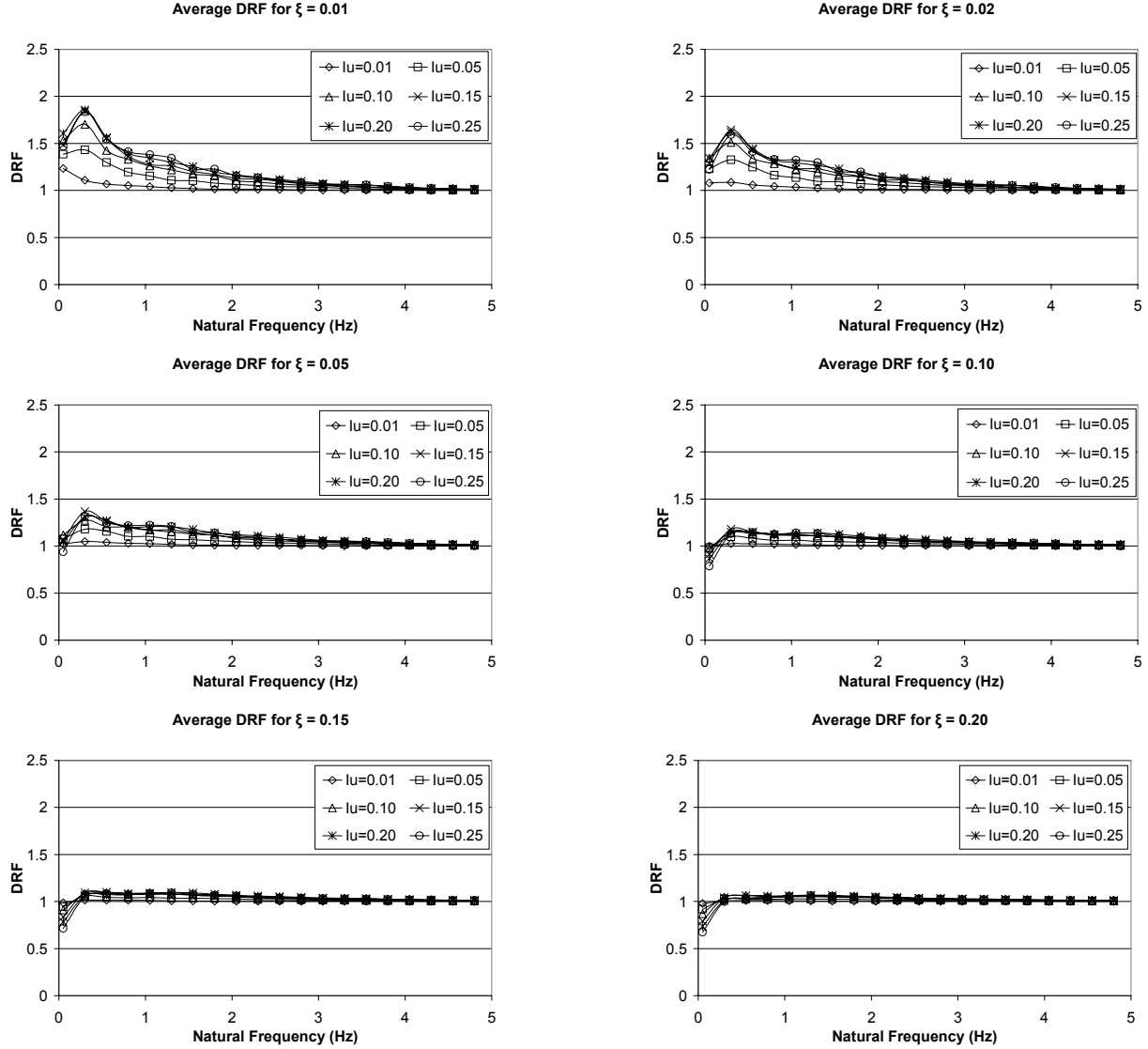


Figure 4: Maximum and averaged DRF of the SDOF system with varied structural characteristics, subjected to a simulated boundary layer wind with variable turbulence intensity

In general terms, greater levels of turbulence lead to greater dynamic response, and less damping lead to greater dynamic response. The largest responses of the systems generally occurred at natural frequencies of 0.05Hz or 0.3Hz. The largest individual DRF observed was 2.44 for  $f_n=0.05\text{Hz}$ ,  $\xi=0.01$  and  $I_u=0.25$ . Interestingly, when the DRFs for the individual storms were ensemble averaged, the maximum response for each given damping and turbulence occurred at  $f_n=0.30\text{Hz}$ . The averaged DRF showed less variation between the higher levels of turbulence than for the lower levels, peaking at approximately 1.85 for  $\xi=0.01$  and  $I_u=0.25$ , 0.20 and 0.15.

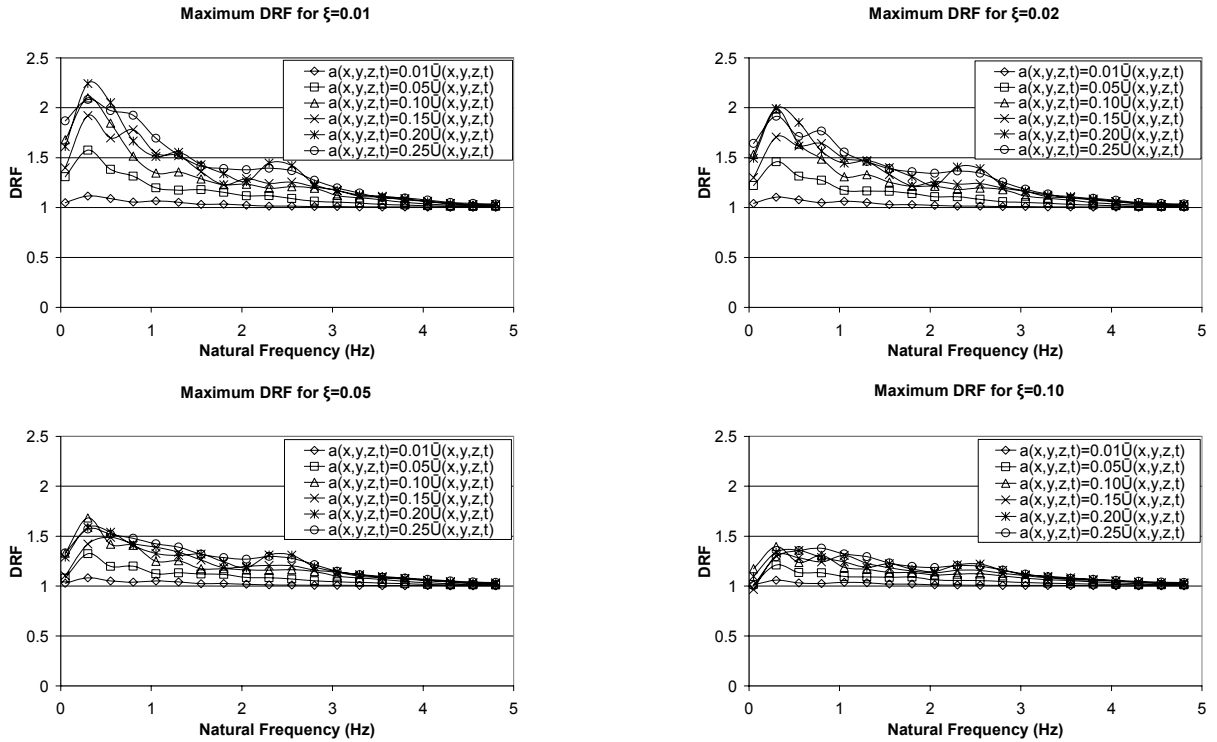
Next, a series of downburst events with comparable characteristics were simulated. A variety of values for  $a(x,y,z,t)$  (Equation 5) were used to produce similar levels of turbulence to those used for the BL wind simulations.  $z_m$  and  $r_t$  were held constant through-out the

simulations with values of 50m and 1500m respectively. A translational speed of  $U_{trans}=10\text{m/s}$  was used. The maximum radial wind speed was varied in conjunction with  $a(x,y,z,t)$  in order to produce the desired 10m gust speed of  $50\pm 2.5\text{m/s}$  (Table 2).

Table 2: Amplitude modulations factor (turbulence intensity equivalent) versus maximum radial wind speed at  $z_m$  for the analytical model downburst simulations

$a(x,y,z,t)$	$\bar{U}_{r,max}$
$0.01 \bar{U}(x,y,z,t)$	73 m/s
$0.05 \bar{U}(x,y,z,t)$	64 m/s
$0.10 \bar{U}(x,y,z,t)$	56 m/s
$0.15 \bar{U}(x,y,z,t)$	48 m/s
$0.20 \bar{U}(x,y,z,t)$	43 m/s
$0.25 \bar{U}(x,y,z,t)$	37 m/s

Similar to the boundary layer tests, 20 storms for each scenario were generated. The simulated wind speed time histories were then applied to the SDOF system under the same range of natural frequencies and critical damping ratios as per the BL tests. The results are shown below.



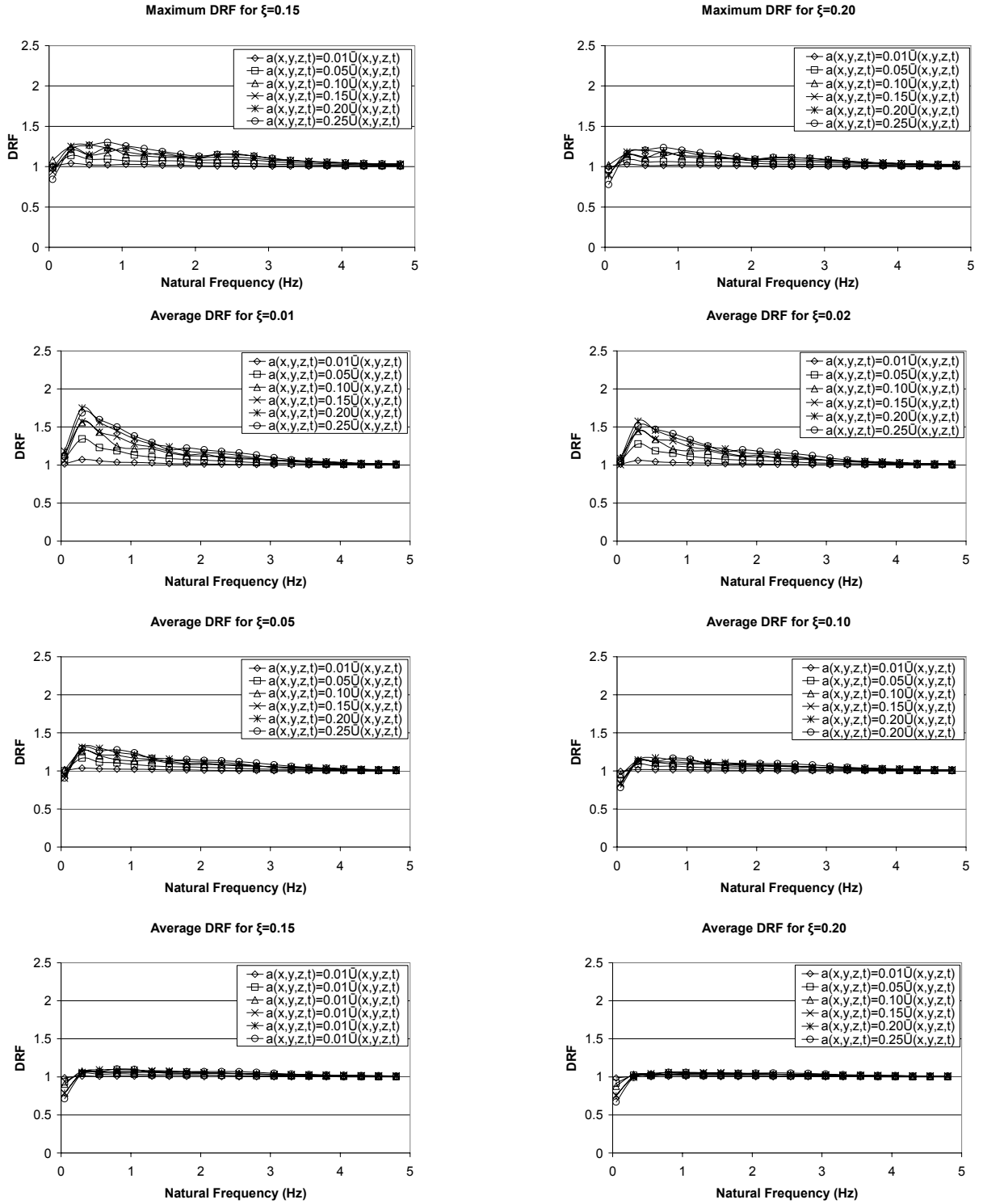


Figure 5: Maximum and averaged DRF of the SDOF system with varied structural characteristics, subjected to a simulated downburst wind with variable turbulence intensity



Similar to the boundary layer winds, less damping and more turbulence generally lead to greater dynamic response. The dynamic response that the simulated downburst created appears to be generally lower than that during the BL winds for natural frequencies below 1Hz. To quantify this, the averaged DRFs for the downburst scenarios were divided by the corresponding averaged DRFs during the BL winds (i.e. the downburst DRF at a given turbulence intensity and damping ratio was divided by the DRF in a BL wind with the same turbulence intensity and damping ratio).

$$DRF \text{ Ratio} = \frac{\text{Average } DRF_{\text{Downburst}}}{\text{Average } DRF_{\text{Boundary Layer}}} \quad (8)$$

The DRF ratio tended to be below 1 for frequencies lower than approximately 1Hz (as low as DRF Ratio=0.71), and the ratios were lowest for cases in which the overall DRF was largest. Results are shown below in Figure 6:

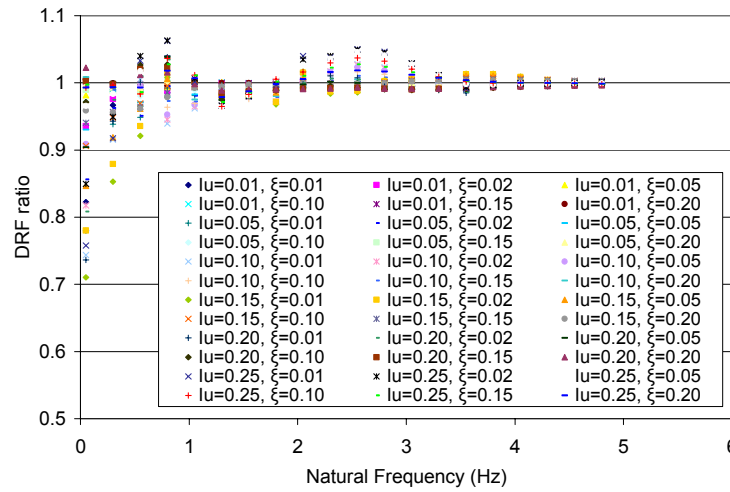


Figure 6: DRF ratio comparison for varied damping, natural frequency and turbulence intensity for downburst and boundary layer winds

Shown below is an example of a wind speed time history and a corresponding displacement time history for a case in which  $a(x,y,z,t) = 0.15 \bar{U}(x,y,z,t)$ ,  $\xi=0.01$  and  $f_n=0.25\text{Hz}$ . Note that although the winds achieve similar peak speeds, the displacement is significantly higher during the boundary layer event.

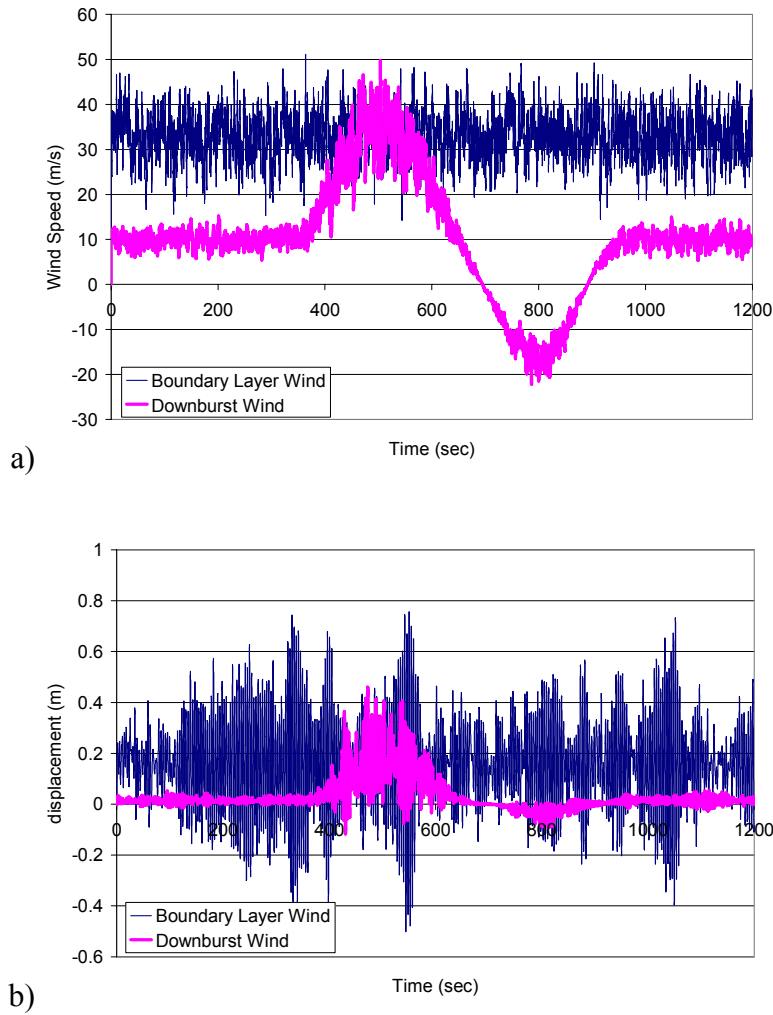


Figure 7: Comparison of a) wind speed time histories and b) displacement response time histories for simulated boundary layer and downburst wind events for the SDOF system with  $f_n = 0.25\text{Hz}$

There appears to be two primary causes for the reduced level of response during the downburst events. During a boundary layer event, the storm maintains the conditions required for peak excitation for a considerable period of time (in this study, 10min). However, during the downburst event, these conditions last for only a brief period of time. The systems modelled with the lower natural frequencies do not appear to have sufficient time to develop a true resonant response to the downburst event. Further, from a probabilistic point of view, we can see in the above figure that the boundary layer winds produce periods of relatively high and low excitation. If the peak winds of the downburst were to coincide with turbulence conditions that would lead to low excitation, then the response due to the downburst event would be quite low. Note that large scale pulsing of the non-turbulent wind speeds was too slow to create any elevated level of dynamic response in itself. The period of the most flexible structure

considered is 20sec, whereas the large sine wave-like pulsing of the storm has a period of approximately 600sec.

For all twenty storms of both the boundary layer winds and the downburst winds, the power spectrum was analysed for the 2048 points (81.92 seconds) around the time of the peak displacement. The base 10 logarithm of the spectrum was calculated and an ensemble average was used to evaluate the ‘mean’ spectrum. Figure 8 shows a comparison of the spectrum for the two types of wind.

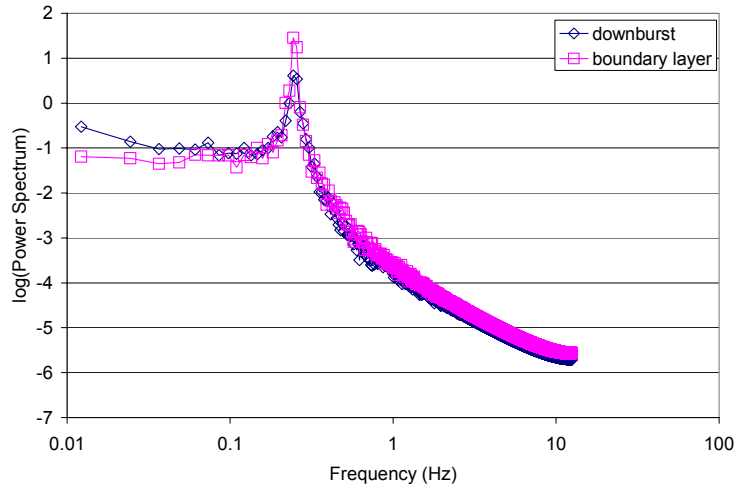


Figure 8: Comparison of the ensemble averaged power spectra of the displacement time history for simulated downburst and boundary layer events for the SDOF system with  $f_n = 0.25\text{Hz}$

The response power spectrum of the downburst is slightly higher below the natural frequency of the structure, and slightly lower for higher frequencies. There is a significant difference in the intensity of the response at the natural frequency of the structure (the log of the downburst response power spectrum was 0.61 versus 1.45 for the log of the BL power spectrum). This difference was apparent even when the two cases were normalised by their respective loading spectra, which varied slightly. This would suggest that the resonant response of the structure is less during the downburst event than during the boundary layer event. Perhaps the reduced time at which high intensity winds occur during downbursts prevent the true development of resonance in the oscillating structure.

The same series of storms was applied to a structure with a  $\xi=0.01$  and  $f_n=2.5\text{Hz}$ . The overall response for the two wind types was very similar. An example of the displacement time history is shown below in Figure 9. Note that the overall level of response for these conditions was significantly lower than for  $f_n=0.25\text{Hz}$ .

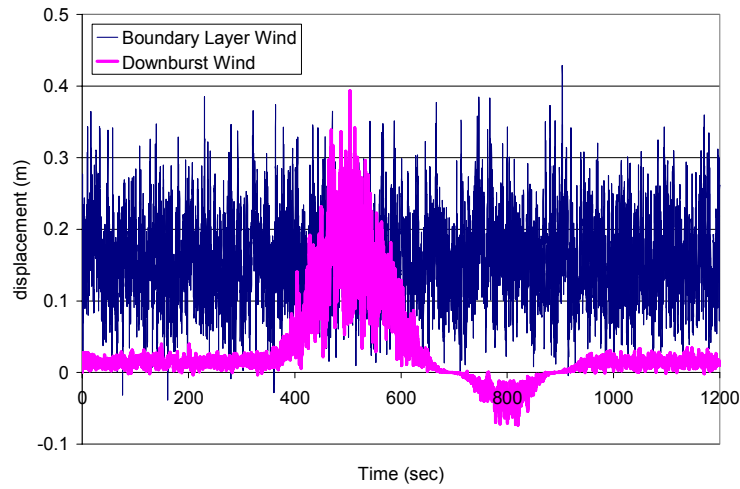


Figure 9: Comparison of the displacement time histories for simulated downburst and boundary layer events for the SDOF system with  $f_n = 2.5\text{Hz}$

The displacement response power spectrum is shown below in Figure 10. The spectra are very similar for the two types of event. The response at the natural frequency is also quite similar, although still slightly lower for the downburst. It appears that for the higher natural frequency, there is sufficient time at the higher wind speeds during the downburst for the resonant response to develop to a comparable level to that seen during the boundary layer winds. Also, due to the lower energy level at which the resonant response is occurring, any variations have less impact on the overall level of response.

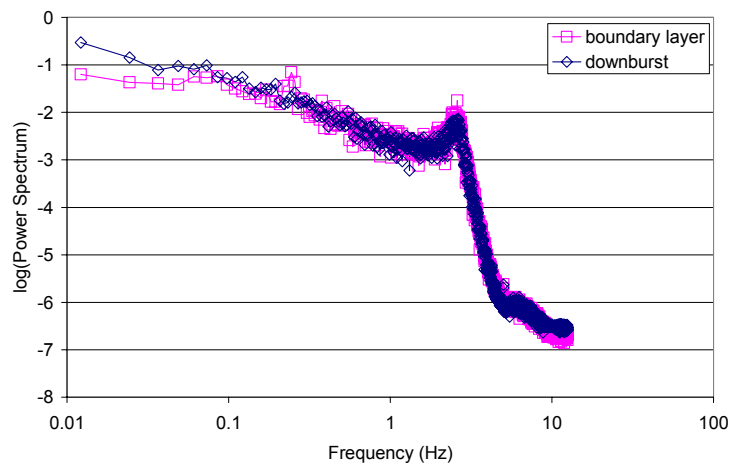


Figure 10: Comparison of the ensemble averaged power spectra of the displacement time history for simulated downburst and boundary layer events for the SDOF system with  $f_n = 2.5\text{Hz}$

From this result, we can say that the duration of the peak wind speeds during a downburst are likely to have a significant impact on the level of response for structures with a low natural frequency. So what factors impact upon the duration of the peak speeds? One such factor is the radius to maximum wind speed. An event with a larger  $r_t$  will, under the current model, be physically larger and therefore produce a more prolonged period of strong gustiness.

#### Variation in the physical size of the downburst

Downburst events with  $50 \pm 2.5$  m/s peak gust speeds were simulated for  $a(x,y,z,t) = 0.10 \bar{U}(x,y,z,t)$ ,  $r_t = 750$  m, 1000 m, 1250 m and 2000 m, and a variety of damping ratios under similar conditions to those used previously. Figure 11 shows examples of wind speed time histories for the various downburst sizes.

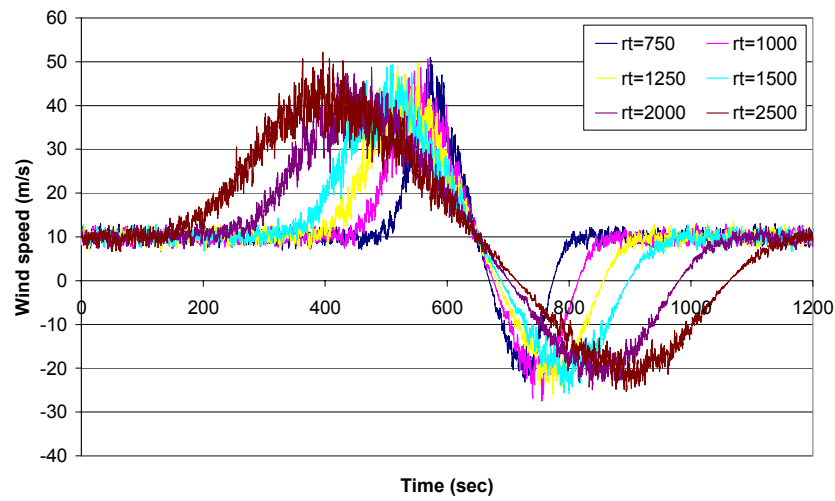
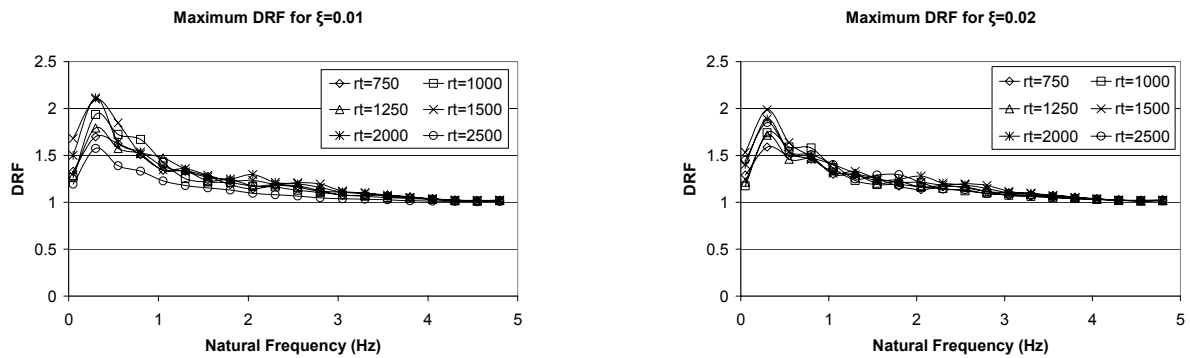
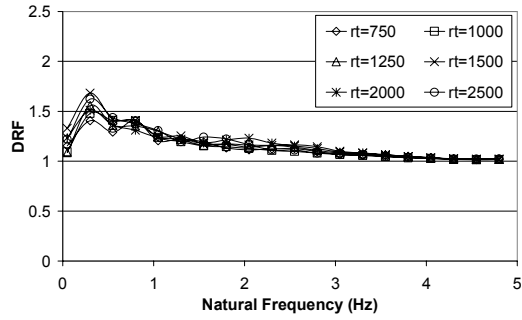


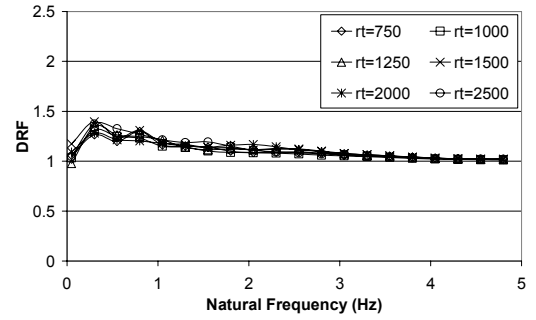
Figure 11: Comparison of wind speed time histories for simulated downbursts with varied radii to maximum wind speed



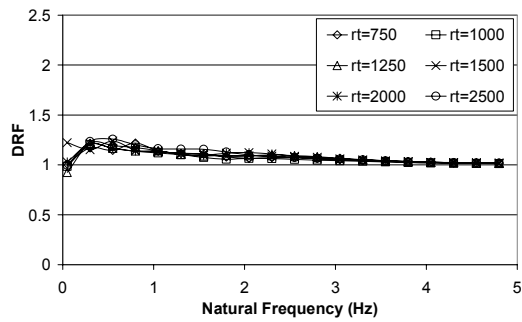
Maximum DRF for  $\xi=0.05$



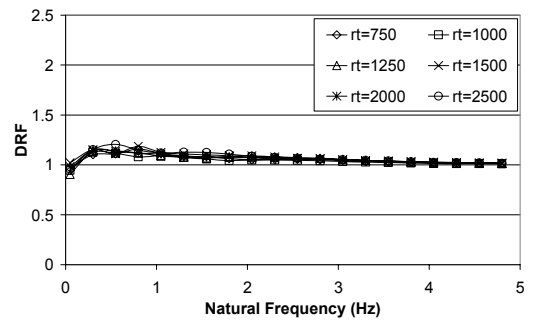
Maximum DRF for  $\xi=0.10$



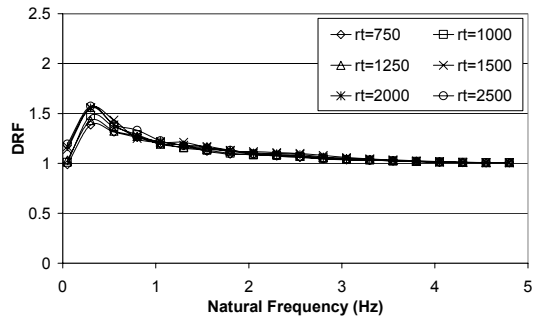
Maximum DRF for  $\xi=0.15$



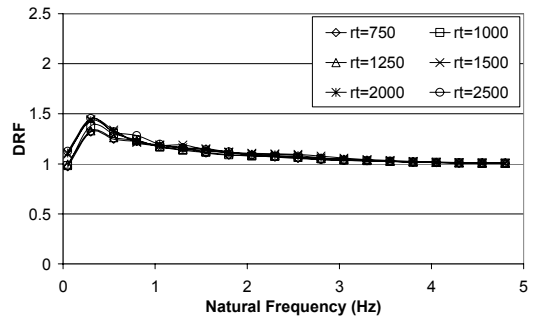
Maximum DRF for  $\xi=0.20$



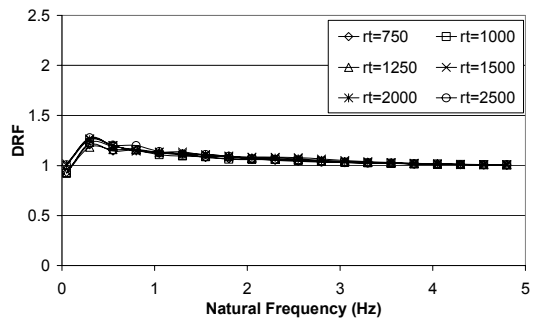
Average DRF for  $\xi=0.01$



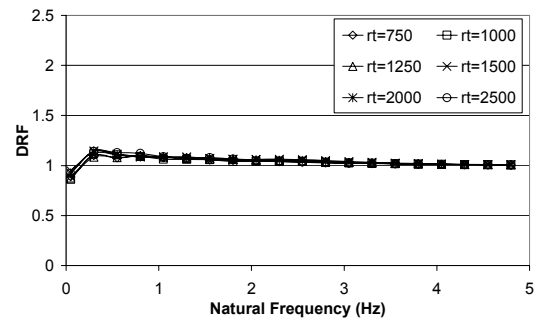
Average DRF for  $\xi=0.02$



Average DRF for  $\xi=0.05$



Average DRF for  $\xi=0.10$



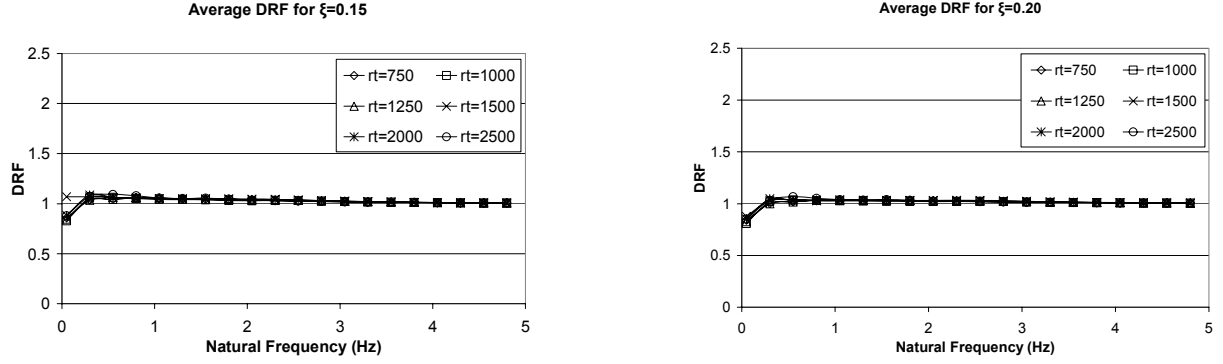


Figure 12: Maximum and averaged DRF of the SDOF system with varied structural characteristics, subjected to a variety of simulated downburst winds for events with varied physical size

As Figure 12 shows, there is a general trend towards an increased level of dynamic response as radius to maximum wind speed increases (an averaged DRF of 1.39 for  $r_t=750\text{m}$  versus 1.57 for  $r_t=2500\text{m}$  when  $\xi=0.01$  and  $f_n=0.30\text{Hz}$ ), although this was not always the case. The difference is again most likely caused by the prolonged duration of the peak gust wind speeds caused by the larger physical size of the event. The power spectra of the displacement time histories are shown in Figure 13 for  $f_n=0.25\text{Hz}$ ,  $a(x,y,z,t)=0.10\bar{U}(x,y,z,t)$  and  $\xi=0.01$ . Although the spectra are quiet similar, the response at the natural frequency shows a small degree of variation following the same generalised trend of lower response for lower radius. Below the natural frequency response was larger as radius decrease. Above the natural frequency the response varied in an inconsistent fashion. Note that the response at the natural frequency for all downburst events was significantly lower than the boundary layer wind.

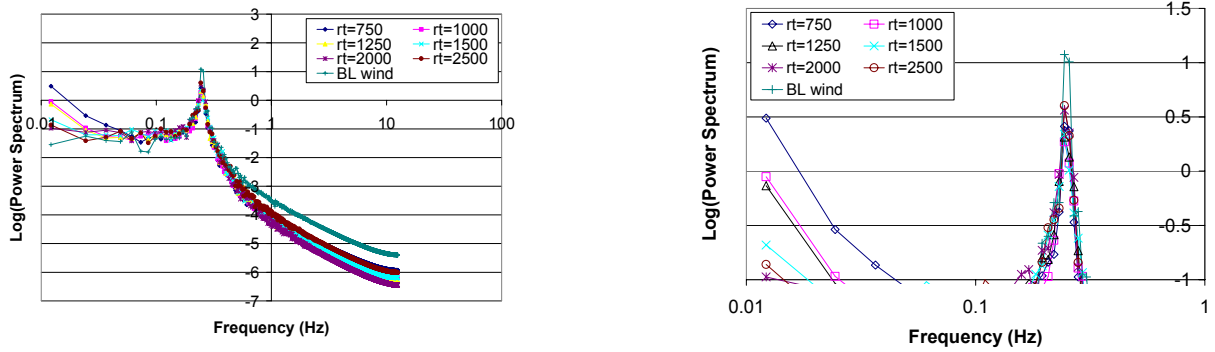


Figure 13: Comparison of the ensemble averaged power spectrums of the displacement time history for simulated downburst and boundary layer events for the SDOF system with  $f_n=2.5\text{Hz}$

## CASE STUDY: SIMULATED AAFB DOWNBURST

The numerical/analytical model described above was used to simulate the 1983 Andrews Air Force Base downburst (Fujita 1983). The downburst took place during mid afternoon on the

1<sup>st</sup> of August 1983, and reached wind speeds of 67m/s shortly after Air Force One landed at the airport.

The event was simulated 20 times using  $U_{max}=120\text{m/s}$ ,  $U_{trans}=8\text{m/s}$ ,  $z_m=80\text{m}$ ,  $a(x,y,z,t) = 0.1$ , and  $r_t$  equal to 700m at the start of the event and increasing linearly at 30m per minute. The intensity factor was given by:

$$\Pi = \begin{cases} \frac{t}{2.75} & 0 \leq t \leq 2.75 \\ e^{\frac{-(t-2.75)}{25}} & t > 2.75 \end{cases} \quad (9)$$

where  $t$  is the time after the start of the event in minutes, which was approximately 11 minutes (660s). Note that direction was excluded from the simulation due to the difficulty associated with transcribing the full-scale wind speed directions. This omission is believed to have no impact on the peak dynamic response of the system, as in all previous simulations the peak response has occurred during the initial peak in wind speeds. An example of a simulated wind speed time history under these conditions is shown in Figure 14.

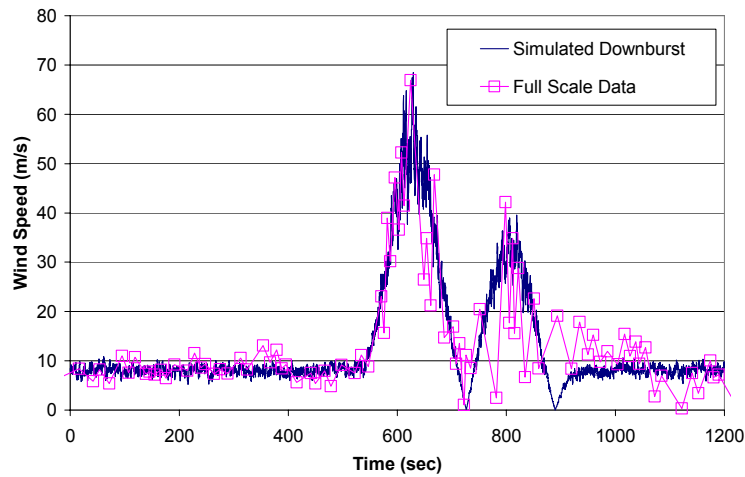


Figure 14: Comparison of the simulated and actual wind speed time histories of the AAFB downburst

The shown below (Figure 15) are the average and maximum DRFs for the SDOF system of a generalised case (analytically modelled with gust speed of  $50 \pm 2.5\text{m/s}$ ,  $r_t=1500\text{m}$  and  $a(x,y,z,t)=0.10\bar{U}(x,y,z,t)$ ). Figure 16 shows the DRF ratio, which in this case is the average DRF for the simulated AAFB wind speed time histories divided by the average DRF for the generalized case.



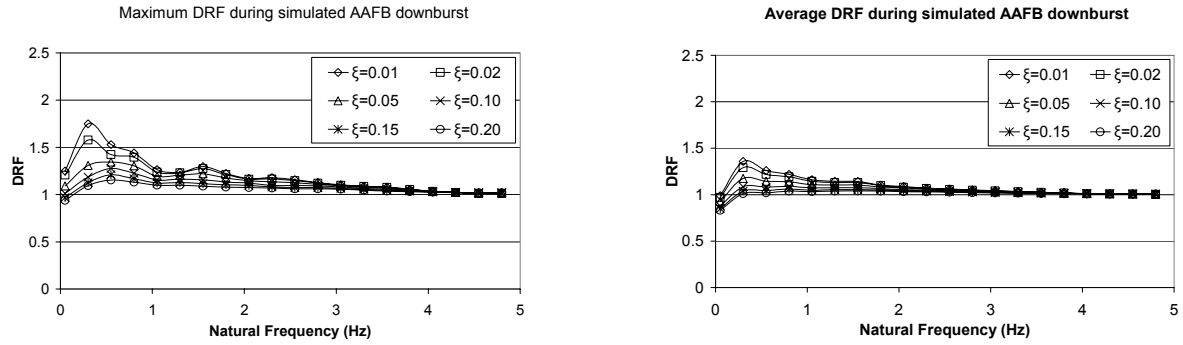


Figure 15: Maximum and averaged DRF of the SDOF system with varied structural characteristics, subjected to the simulated AAFB downburst winds

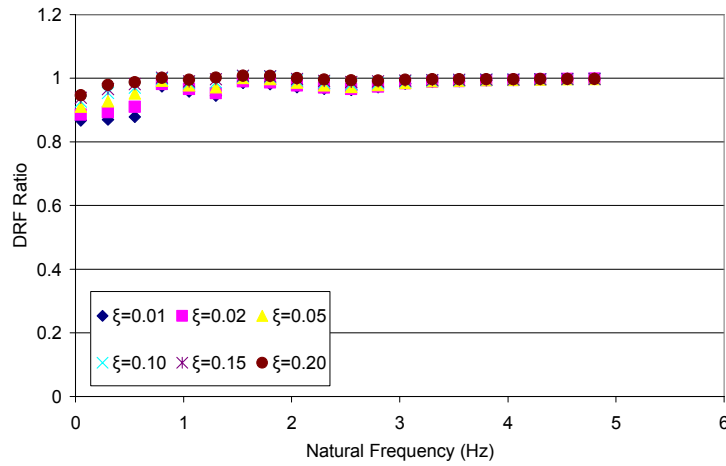


Figure 16: DRF ratio comparison for the simulated AAFB winds and a generalised downburst

The response of the SDOF system to the simulated AAFB downburst can be characterised in these general terms; the response of the system was typically lower under the action of the AAFB downburst than the generalised downburst for low natural frequencies ( $<1\text{Hz}$ ), and was similar for higher natural frequencies. The averaged maximum dynamic response of the system to the AAFB storm was as much as 13% lower than that for the generalised downburst. These observations are consistent with the results of the varied radius to maximum wind speed tests. The simulated AAFB storm had a significantly lower radius to peak wind speed (700m at the start of the event and increasing linearly at 30m per minute) than the generalised downburst (constant 1500m throughout the event), and as such would be expected to produce a lower dynamic response than the generalised downburst for reasons discussed earlier in this paper.

## CONCLUSIONS

A number of generalised trends were observed during the testing described above, which can be described as:

- The dynamic response of a SDOF system appears to be the same or lower than that caused by a boundary layer wind with similar characteristics. For higher natural frequencies there was little difference between the DRF of the BL and downburst winds. For low natural frequencies and low damping ratios, the downburst winds produced a lower level of maximum excitation.
- In cases in which the response was lower in the downburst winds, it may be that there is a reduced level of resonant response, possibly due to the reduced period of time for which the high wind speeds act, as compared to the 'stationary' boundary layer winds. Probabilistically, due to the brief nature of a downburst, turbulence conditions that would result in a relatively low level of excitation can exist for the entire duration of the severe wind speeds, resulting in a lower average level of response for a large number of events with a given gust speed.
- Physically smaller downburst events appear to produce the same or lower dynamic response than physically larger events, for the reasons described in point two.

Further work is required to investigate the manner in which complex structures respond dynamically to downburst winds. However, the general trends described here indicate that downburst winds are less likely to cause structural damage than a boundary layer style winds. Despite this, there are numerous instances in which structures designed to withstand boundary layer style winds have been damaged or destroyed during downburst events. The results of the study return some of the focus of future work to characterising the static loading conditions imposed on a structure during a downburst, be it the design gust speed for a given return period, the correlation of load over a large span, the manner in surface level downburst winds are affected by complex terrain, or the loading imposed on a bluff body structure.

## REFERENCES

Chay, M. T., Albermani, F. and Wilson, R. (2005). "Numerical and analytical simulation of downbursts for investigating dynamic response of structures in the time domain". *Article in Press - Engineering Structures*.

Chen, L. and Letchford, C.W. (2004) "A deterministic-stochastic hybrid model of downbursts and its impact on a cantilever structure". *Engineering Structures*, Vol. 26, 619-626.

Chen, L. and Letchford, C.W. (2005) "Simulation of Extreme Winds from Thunderstorm Downbursts" *Proceedings of the Tenth Americas Conference on Wind Engineering*, May 31-June 4 2005, Baton Rouge, Louisiana, USA.

Choi,

Fujita, T.T. (1990). "Downbursts: Meteorological Features and Wind Field Characteristics". *Journal of Wind Engineering and Industrial Aerodynamics*, Vol. 36, 75-86.

Kaimal, J.C., Wyngaard, J.C., Izumi, Y. and Cote, O.R. (1972). "Spectral Characteristics of surface-layer turbulence". *Quarterly Journal of the Royal Meteorological Society* Vol. 98, 563-589.

Paz, M. (1997). *Structural Dynamics - Theory and Computation*. Chapman and Hall, New York.

Samaras, E., Shinozuka, M., and Tsurui, A. (1985). "ARMA Representation of Random Processes". *Journal of Engineering Mechanics*, Vol. 111(3), 449-461.